

Does the continuum theory of dynamic fracture work?

David A. Kessler

Department of Physics, Bar-Ilan University, Ramat-Gan, Israel

Herbert Levine

Department of Physics, University of California, San Diego, La Jolla, CA 92093-0319

(Dated: October 24, 2018)

We investigate the validity of the Linear Elastic Fracture Mechanics approach to dynamic fracture. We first test the predictions in a lattice simulation, using a formula of Eshelby for the time-dependent Stress Intensity Factor. Excellent agreement with the theory is found. We then use the same method to analyze the experiment of Sharon and Fineberg. The data here is not consistent with the theoretical expectation.

PACS numbers:

Recently, there has been renewed interest in the physics community concerning the problem of dynamic fracture. This interest was kindled by experiments[1, 2] showing a universal transition to crack branching and the realization that one could not approach this question within the confines of traditional fracture mechanics[3]. Since then, there have been other novel experimental findings[4] as well as further evidence of theoretical inadequacies.

In the standard approach, (see, for example, [5]) dubbed Linear Elastic Fracture Mechanics, one assumes that continuum elasticity is valid everywhere outside of an microscopically sized process zone. The instantaneous crack tip velocity is then postulated to depend only on the singular part of the stress field obtained by solving this macroscopic continuum problem. This singularity of the stress field is universal in nature, up to an overall multiplicative factor, the so-called stress-intensity factor (SIF). Even if there is a well-defined relationship between the crack velocity and the SIF, the theory cannot predict the form of the relationship, as that depends explicitly on physics at the scale of the process zone. As realized initially by Slepyan[6], one way to remedy this deficiency is to model the entire system as a lattice of mass points connected by nonlinear springs. On scales large compared to the lattice spacing, the displacement approaches that predicted by the continuum theory; on the scale of the crack tip, the stress field divergence is regularized, thereby allowing for the imposition of a physically sensible breaking criterion. This criterion is usually in the form of a critical spring displacement, as this allows for the possibility of analytical solutions of the model[7, 8, 9, 10, 11, 12].

Thus, the lattice model provides a self-consistent realization of the basic assumption underlying engineering fracture mechanics, the ability to separate the linear elasticity calculation from the microscopic physics controlling the tip. In general, however, it is hard to test the LEFM since it is difficult to reliably measure the SIF in a lattice calculation, as this requires an extremely (and imprac-

tically) large system. Only then is there an appreciable range of scales in which one is sufficiently far from the crack tip that lattice effects are unimportant and sufficiently close that the fairly weak square-root singularity dominates. However, for the case of a crack accelerating from rest, the approach of Kostrov [13] and Eshelby [14] provides an analytic prediction of the SIF, independent of the details of the dynamics. With this first-principles determination of the SIF, it is possible to test the LEFM picture. Specifically, we will show that in the lattice model, in accord with expectations, the stress intensity factor governing the strength of the stress singularity is the only information passed from the macroscopic field to the process-zone dynamics of the crack tip. In fact, this separation is quantitatively accurate even for rather small lattices where one might have questioned the efficacy of the continuum approach. Moreover, these results allow us to construct a test of the theory based on the actual fracture data presented by Sharon and Fineberg[15] for the same case of a crack accelerating from rest. Here, however, the data do not appear to conform to theoretical expectations. At the end, we discuss possible implications of this failure.

We begin with the lattice model. We work with a 2d square lattice with unit spacing between the mass points. These masses are coupled via both nearest neighbor and next-nearest neighbor ideally brittle central force springs with spring constants k_1 and k_2 respectively. It is easy to show that with the choice $k_1 = 2k_2 = 2\mu = 2\lambda_{2d}$, the continuum linear elastic limit of this model is isotropic with the aforementioned Lamé' constants; hence the Poisson ratio $\nu_{2d} = 1/4$. We will assume that the actual 3d system exhibits plane stress and so can be approximated via a 2d system with

$$\lambda_{2d} = \frac{2\mu\lambda}{2\mu + \lambda};$$

the actual Poisson ratio of the material being modeled is $\nu = \nu_{2d}/(1 - \nu_{2d}) = 1/3$. The dynamics arising from this force is taken to include the possibility of a Kelvin

viscosity term. The final equation of motion is therefore

$$\frac{\partial^2 \vec{u}(\vec{x})}{\partial t^2} = \left(1 + \eta \frac{\partial}{\partial t} \right) \left[\frac{k_1}{2} \sum_{\hat{n} \in nn} ((\vec{u}(\vec{x} + \hat{n}) - \vec{u}(\vec{x})) \cdot \hat{n}) \hat{n} + \frac{k_2}{2} \sum_{\hat{n} \in nnn} ((\vec{u}(\vec{x} + \hat{n}) - \vec{u}(\vec{x})) \cdot \hat{n}) \hat{n} \right] \quad (1)$$

As discussed in [8, 16], the damping due to nonzero Kelvin viscosity occurs only inside the process zone if η is chosen $O(1)$. Finally, any bond whose length goes above a breaking threshold, which we take to be 1, has its spring constant set to zero.

As discussed above, we study in detail a finite length crack accelerating from rest. Initially, a crack is placed along the mid-line of a sample (here between rows 0 and 1 of our lattice), extending a length ℓ_0 from the left edge. The top and bottom rows of the lattice have fixed (and opposite) displacements $\vec{u} = \Delta \hat{y}$ and the lateral edges are free. The loading is chosen to be just below the critical value at which the crack will start to propagate; since this loading is a decreasing function of crack length, a crack with one additional broken bond will in fact start to elongate. The system is then allowed to fully relax to its equilibrium stress state; this is accomplished via a multigrid technique described in detail elsewhere[17]. Once this is done, an additional bond is broken by hand (i.e., its spring constant is set to zero; no actual displacement of particles is involved) and the crack tip accelerates. As it moves, we monitor the bonds across the crack surface $y = 1/2$. When all three bonds attached to a given point $\vec{x} = (x, 1)$ break, the crack length is deemed to have increased by one and the velocity at that time is measured as the inverse of the time interval since the last such event. We do not allow bonds off the crack line to break, thereby suppressing any possible branching instabilities. We also enforce symmetry across the crack surface, simulating only the upper half of the lattice. Each run is characterized by the transverse lattice size W , the initial length of the crack ℓ_0 , damping constant η and the driving displacement Δ . Typical data generated by this procedure for both the undamped and highly damped cases are presented in Fig. 1.

According to the classic calculation by Eshelby [14], the stress intensity factor, K , or equivalently the Eshelby B factor (which is a constant multiple of K), at the progressing crack tip for a system that starts in equilibrium can, up to a certain time, be written as a product of two factors:

$$B_I(t) = A(v(t)) \int_{\ell_0}^{\ell(t)} dx \frac{\sigma_{eq}^{yy}(x)}{\sqrt{x - \ell_0}} \quad (2)$$

Here σ_{eq}^{yy} is the normal stress on the mid-line $y = 1/2$ as found from the equilibrium stress field; it diverges of course near the edge of the equilibrium crack $x = \ell_0$ with a static stress intensity factor. The first factor $A(v)$

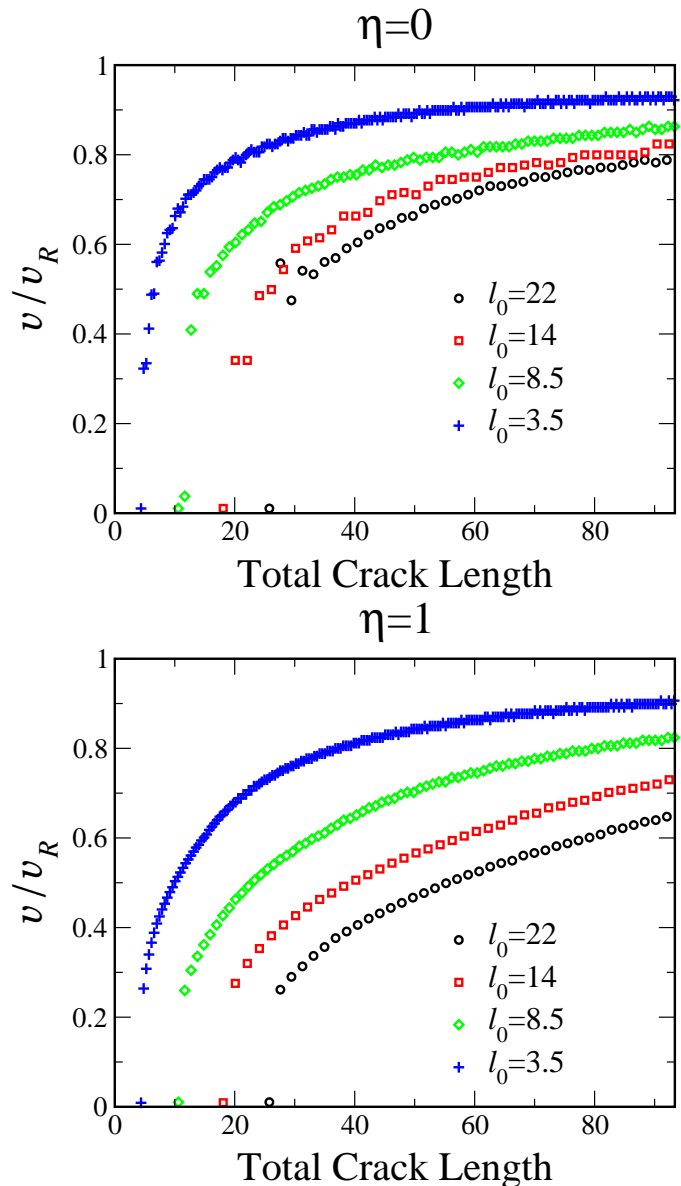


FIG. 1: Simulation results for velocity vs. crack length for various initial seed cracks. The system widths, W , in lattice units are 239, 219, 415, and 1004 for the four runs for decreasing ℓ_0 . For later convenience, all lengths in the graph are scaled by a factor $440/W$. Velocities are normalized to the Rayleigh velocity.

depends only on the *instantaneous* velocity at time t and the second factor (which we will refer to as B_0) depends on time only through the *instantaneous* crack length $\ell(t)$. This equation holds true as long as sound waves reflected from the boundaries have not interacted with the crack tip. There are two boundaries one must be concerned with, the lateral boundaries at $y = \pm W/2$ and the edge at $x = 0$. We take care that all our data come from times before these interactions occur.

Now, if the true microscopic breaking events only cou-

ple to the macroscopic field via B_I , we expect that there will be some fixed relationship between the tip velocity and this number. Usually, this relationship is considered to arise due to energy conservation and is therefore written as an equality of the energy flux into the tip and the energy necessary to break bonds along a unit length of crack

$$\Gamma(v) = f(v)B_I^2 \quad (3)$$

Here f is a complicated but explicit function and Γ is the breaking energy. In fact, Γ can be determined via the dependence of steady-state cracks on the driving load and thereafter used for the accelerating crack case. For our purposes, this hypothesis leads to the existence of a universal relationship, independent of W , Δ and ℓ_0 (but dependent on η), between the measured velocity $v(t)$ and the Eshelby function $B_0(\ell(t))$.

To test this strong prediction of LEFM, we use our lattice model simulations discussed above. We calculate the integral in Eq. (2) by replacing the continuum stress with its lattice analog (defining $\vec{u} \equiv (u, v)$)

$$\sigma_{eq}^{yy}(x) = -k_1 v_{eq}(x, 0) - \frac{1}{2}k_2 [u_{eq}(x-1, 0) - u_{eq}(x+1, 0) + v_{eq}(x-1, 0) + v_{eq}(x+1, 0)] \quad (4)$$

The fields that enter are the equilibrium fields present before the crack tip begins to move. The integral is then replaced by a sum, taking care to resolve the singularities in the integrand. This yields a function $B_0(\ell; W, \ell_0)$ which can be plotted versus the velocity. The results of this exercise are presented in Fig. 2, demonstrating almost perfect data collapse even for fairly small transverse sizes W .

So, the lattice model does indeed serve as an instantiation of the LEFM picture developed by the fracture community for straight accelerating cracks. But now, we can use the Eshelby B_0 function calculated as just described to process actual crack velocity/length data from the experiments on PMMA carried out by Sharon and Fineberg. This data comes from a protocol very similar to what we used above in which the loading is set to a point where a touch of razor blade will cause the rapid elongation of a previously created notch in the material. For PMMA, the elastic constants are $\lambda = 2680 MPa$, $\mu = MPa$, giving $\nu = .35$. Going to the plane stress case leads to an effective Poisson ratio $\nu_{2d} \simeq .259$ which is very close to the value forced upon us by the restriction to n.n. and n.n.n. central forces. We did check that generalizing our model to include bond-bending springs and thereby obtaining the precise value of the Poisson ratio did not alter in any way the results which we will now present.

In fact, we designed our simulation to mimic as closely as possible the experimental situation. Thus, not only were the elastic constants chosen appropriately, the aspect ratio was also fixed to that of the experiment (

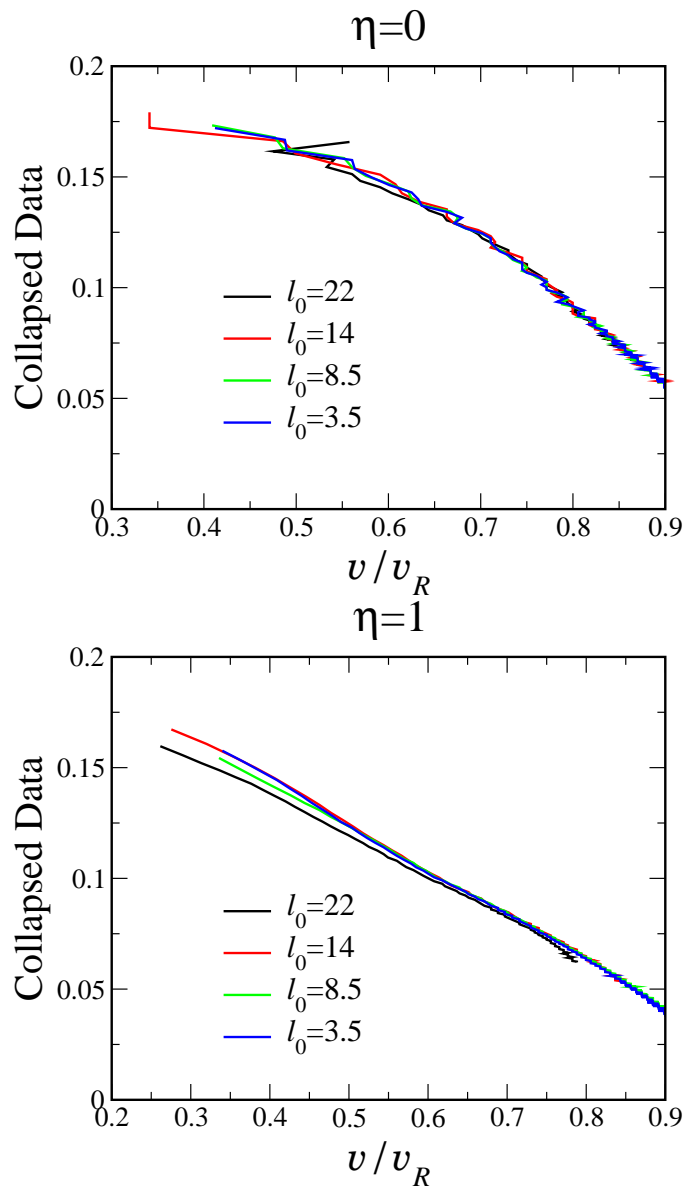


FIG. 2: Eshelby data collapse for $\eta = 0, 1$ for the runs shown in Fig. 1. Notice the slight systematic dependence on ℓ_0 for the $\eta = 1$ data, presumably arising from the larger process zone in this case [9].

a width of 440 mm. and a length of 380 mm.). The lengths of the initial seed cracks were also chosen to be in the same ratio to the width as in the experiment. This constraint fixed our choice of the actual width in lattice units, as we wanted the initial crack to be large (of order 10) on the lattice scale.

Fig. 3 shows our attempt to verify the continuum hypothesis for the PMMA data. In our opinion, the data are quite convincingly inconsistent with the universality of the $v - B_0$ relationship. Note that this is the opposite conclusion from that reached by the experimenters themselves, as discussed in Ref. [15]. There, the exact

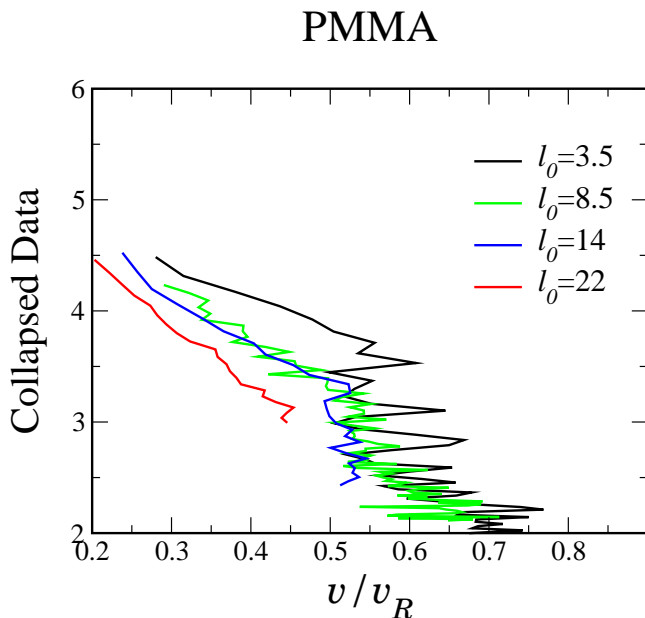


FIG. 3: Attempted data collapse for the Sharon-Fineberg PMMA experiment. Initial crack lengths are given in mm.

Eshelby function was replaced by an approximate form based on the *static* stress intensity factor for a crack of length $\ell(t)$. Note that these functions while close for $\ell \approx \ell_0$, become quite different for larger length cracks. The static stress intensity factor saturates for $\ell \gg W/2$, whereas the exact Eshelby function increases linearly in this regime. We have checked that the use of this approximation happens to push the data into closer agreement with the theory and could lead to a mistaken impression of data collapse. This does not happen with the exact expression and conversely the approximate form does not lead to a very good data collapse for the simulation study discussed above. The same situation obtains for the Sharon-Fineberg measurements on fracture in glass (results not shown). There the data collapse is, if anything, even worse.

It should be noted that the agreement between the lattice theory and LEFM is very dependent on our absolute suppression of off-axis cracking. If all bonds are allowed to break, above a critical velocity the crack no longer propagates in a straight line, and the assumptions implicit in the Eshelby calculation of the instantaneous SIF break down completely. At that point, there is no longer any way to reliably measure the SIF and thus test LEFM. Needless to say, LEFM in its simplest formulation does not predict the direction of branching, and thus cannot address to the post-instability dynamics of the crack. The effects of the instability in the experiment (which appear to exhibit different dynamics than in the lattice model in this regime) are clearly visible at later times (larger velocities), but cannot explain the apparent failure of the data collapse at smaller velocities.

The question remains how to explain this failure of LEFM in the Sharon-Fineberg experiment. Putting aside for the moment the obvious possibility of systematic errors in the determination of the velocity or position of the crack, the only explanation that suggests itself is that the process zone is for some reason very large. The monotonic dependence on ℓ_0 , similar to, though much larger than that seen in the $\eta = 1$ simulation, is consistent with this hypothesis. This might be due either to the polymeric nature of the microstructure of the polymer system, the heterogeneity of the small-scale structure, or to the large dissipation in the system. However, given the success of LEFM on our relatively small systems, it is not easy to accept this as a sufficient explanation. Further experiments on other systems are clearly necessary for an unraveling of this conundrum.

The authors wish to thank J. Fineberg and E. Sharon for providing the raw data from their experiment, and for extensive discussions. The work of DAK is supported in part by the Israel Science Foundation. The work of HL is supported in part by the NSF, grant no. DMR-0101793.

-
- [1] J. Fineberg, S. P. Gross, M. Marder and H. L. Swinney, Phys. Rev. Lett. **67**, 457 (1991); Phys. Rev. B **45**, 5146 (1992).
 - [2] E. Sharon and J. Fineberg, Philos. Mag. **78**, 243 (1998).
 - [3] J. Fineberg and M. Marder, Phys. Rep. **313**, 1 (1999).
 - [4] R. D. Deegan, P. J. Petersan, M. Marder, and H. L. Swinney, Phys. Rev. Lett. **88**, 014304 (2002).
 - [5] K. B. Broberg, “Cracks and Fracture”, (Academic Press, 1999, San Diego).
 - [6] L. I. Slepyan, Doklady Akademii Nauk SSSR **258** 561 (1981) [Sov. Phys. Dokl. **26**, 538 (1981)]; Sh. A. Kulamekhtova, V. A. Saraikin, and L. I. Slepyan, Izv. AN SSSR. Mekhanika Tverdogo Tela, **19**, 112 (1984) [Mech. Solids **19**, 102 (1984)].
 - [7] M. Marder and S. P. Gross, J. Mech. Phys. Solids **43** 1 (1995).
 - [8] D. A. Kessler and H. Levine, Phys. Rev. E **59**, 5154 (1998).
 - [9] D. A. Kessler, Phys. Rev. E **61**, 2348 (2000).
 - [10] L. Pechenik, D. A. Kessler, and H. Levine, Journal of the Mechanics and Physics of Solids **50**, 583 (2002).
 - [11] L. I. Slepyan, M. V. Ayzenburg-Stepanenko, J. P. Dempsey, Mechanics of Time-Dependent Materials **3**, 159 (1999).
 - [12] E. Gerde and M. Marder, Nature **417**, 285 (2001).
 - [13] B. V. Kostrov, Prikladnaia Matematika i Mekhanika **30** 1042 (1966) [Applied Math. and Mech. **30**, 1241 (1966)].
 - [14] J. D. Eshelby, J. Mech. Phys. Solids **17**, 177 (1969).
 - [15] E. Sharon and J. Fineberg, Nature **397**, 6717 (1999).
 - [16] J. S. Langer, Phys. Rev. E **46**, 3123 (1992); O. Pla, F. Guinea, E. Louis, S. V. Ghasias, and L. M. Sander, Phys. Rev. B **57**, R13981 (1998).
 - [17] D. A. Kessler and H. Levine, in preparation.